QUANTUM COMPUTATION

Janusz Adamowski

Faculty of Physics and Applied Computer Science
AGH University of Science and Technology, Kraków

2009/2010

Dziękuję Pani Joannie Tomkowicz za pomoc
w opracowaniu internetowej wersji wykładów.

"Information is physical"

Rolf Landauer

Outline of lecture

(1) Brief history of quantum computation

(2) Bits and qubits

(3) Quantum logic gates

(4) Simulation of CNOT gate on coupled quantum dots

(5) Simulation of SWAP gate on spin qubits

(6) Discussion

(7) Summary

1 Brief history of quantum computation

- Paul Benioff (1980): concept of **revertible quantum Turing machine**
- Richard Feynman (1982): suggesting the possibility of **direct application** of quantum laws to quantum computation
- David Deutsch (1985): theory of quantum Turing machine
- Peter Shor (1994): **first effective quantum algorithm** (factorization of large integer numbers performed in polynomial time)
- Lov Grover (1996): quantum algorithm of data base searching (computation time = square root of time of the fastest classical algorithm)
- Wojciech Żurek (former graduate student of Technical Physics at the AGH University of Science and Technology) + Wooters:
  non-cloning theorem: there exists no copy machine to copy the qubits
- Artur Ekert (former graduate student of Jagellonian University): **quantum cryptography**

2 Bits and qubits

2.1 Bit

Bit = unit of information in classical computer science

The physical system with N states can store a quantity Q of information, where

$$Q = \log_2 N \, . \tag{1}$$

If $N = 2^K$, then K bits of information are stored in the system.

2.1.1 Physical realization of bit

Arbitrary physical system with two states. We denote these states as 0 and 1. For example, the $p - n$ junction diode: switched off (0) and switched on (1).

Remarks

- states 0 and 1 of the bit are taken on with probabilities $P_j = 0, 1$ $(j = 0, 1)$
- write/readout process of the bit (switching on/off the diode) requires a flow of $\sim 10^6 \div \sim 10^8$ electrons
  $\Longrightarrow$ **classical macroscopic process**

2.2 Qubit

Qubit = quantum bit

Basis states in two-dimensional Hilbert space:

$$|0\rangle, |1\rangle \in \mathcal{H}^{(2)}$$

$$|\textbf{qubit}\rangle \equiv |\psi\rangle \stackrel{def}{=} a_0|0\rangle + a_1|1\rangle \tag{2}$$

Complex amplitudes a_0, a_1 satisfy the normalization condition

$$|a_0|^2 + |a_1|^2 = 1 \tag{3}$$

It is often said that the qubit is a quantum analogue of classical bit. However, **this analogy is not complete and sometimes misleading.** For example, one can determine the quantity of information in the qubit only if $|\psi\rangle \equiv |j\rangle$, where $j = 0, 1$, in other words, exclusively if the system is in the basis state.

The qubit is a linear combination of basis states

$$|\psi\rangle = a_0|0\rangle + a_1|1\rangle \ ,$$

whereby – in general – $a_0, a_1 \neq 0$.
Therefore, we cannot ascribe definite logical values 0 or 1 to the qubit.

2.2.1 Qubit in spinor representation

Basis states can be written down as spinors

$$|0\rangle = \begin{pmatrix} 1 \\ 0 \end{pmatrix} \ , \quad |1\rangle = \begin{pmatrix} 0 \\ 1 \end{pmatrix} \tag{4}$$

Arbitrary qubit in spinor representation

$$|\psi\rangle = \begin{pmatrix} a_0 \\ a_1 \end{pmatrix} \tag{5}$$

2.2.2 Physical realization of qubits

Physical realization of qubits: arbitrary quantum system with two states.

Examples:

- electron in QD with two bound states
- spin of electron (spin qubit)
- polarized photon

Remarks

- Probability P_j of finding the qubit in certain basis state, e.g., in state $|j\rangle$, $(j = 0, 1)$
$$P_j = |a_j|^2 \leq 1 \tag{6}$$
- Some authors define the qubit as **the two-state quantum system**. In my opinion, however, it is more convenient to treat the qubit as **the mathematical object (state vector in Hilbert space)**. This is also the opinion of Nielsen and Chuang [1].

2.2.3 Two-qubit states

Let us consider the vector space $\mathcal{H}^{(2)} \otimes \mathcal{H}^{(2)}$.
This vector space is spanned on the following basis:

$$|i\rangle \otimes |j\rangle \equiv |ij\rangle \ (i, j = 0, 1) \tag{7}$$

Explicit form of two-qubit basis

$$|00\rangle, |01\rangle, |10\rangle, |11\rangle \tag{8}$$

Arbitrary two-qubit state

$$|\Psi\rangle \stackrel{def}{=} a_{00}|00\rangle + a_{01}|01\rangle + a_{10}|10\rangle + a_{11}|11\rangle \tag{9}$$

where

$$|a_{00}|^2 + |a_{01}|^2 + |a_{10}^2 + |a_{11}|^2 = 1 \tag{10}$$

2.2.4 Bell states (EPR states)

EPR = Einstein, Podolsky, Rosen

$$|\Psi_{00}\rangle = \frac{1}{\sqrt{2}}(|00\rangle + |11\rangle) \ , \tag{11a}$$
$$|\Psi_{01}\rangle = \frac{1}{\sqrt{2}}(|01\rangle + |10\rangle) \ , \tag{11b}$$
$$|\Psi_{10}\rangle = \frac{1}{\sqrt{2}}(|00\rangle - |11\rangle) \ , \tag{11c}$$
$$|\Psi_{11}\rangle = \frac{1}{\sqrt{2}}(|01\rangle - |10\rangle) \ . \tag{11d}$$

Remark

More rigorous notation for Bell states

$$|\Psi_{ij}\rangle = \frac{1}{\sqrt{2}}(|i\rangle_A|j\rangle_B \pm |j\rangle_A|i\rangle_B) \ , \tag{12}$$

[1] M. A. Nielsen and I.L. Chuang, *Quantum Computation and Quantum Information*, Cambridge University Press, Cambridge, UK, 2000)

where A and B are subsystems of two-qubit system AB and $|i\rangle_{A,B}$ and $|j\rangle_{A,B}$ $(i,j=0,1)$ are the one-qubit basis states in subspace A or B.

Properties of Bell states:

(1) The Bell states are **non-separable**,
i.e., $|\Psi_{ij}\rangle \neq |i\rangle|j\rangle$.

(2) The Bell states are **the entangled states = e-bits**.

(3) **Einstein-Podolsky-Rosen (EPR) paradox:**
When measuring one qubit we obtain, **without performing the measurement**, the value of the second qubit.

Comment on property (3)

Let us consider the system AB in state

$$|\Psi_{01}\rangle = \frac{1}{\sqrt{2}}(|0\rangle_A|1\rangle_B + |1\rangle_A|0\rangle_B) \ .$$

Suppose we perform the measurement on subsystem A and obtain eigenvalue λ_A^0, which is associated with state $|\psi\rangle_A = |0\rangle_A$. This means that subsystem A is in state $|0\rangle_A$. Then, **without performing the measurement on subsystem B**, we can ascertain that **subsystem B is in state $|\psi\rangle_B = |1\rangle_B$ with probability 1**.

The authors (EPR) treated the EPR paradox as a proof of contradiction in quantum mechanics.

Recently, we interpret the EPR paradox as a result of **strong quantum correlation** that occurs in the case of interacting (even very weakly interacting) subsystems A and B.

Experimentally, the Bell (EPR) states have been observed for photons at $\sim$ 100 km distance between the source and detector.

The EPR states are widely used in quantum cryptography.

3 Quantum logic gates

Mathematical realization of quantum logic gate (quantum logic operation)

$$|output\rangle = U|input\rangle \ , \tag{13}$$

where U is the unitary operator.
Usually, U is the time evolution operator

$$U \equiv U(t) = e^{-(i/\hbar)Ht} \ , \tag{14}$$

where H = Hamiltonian of the system.

3.1 Physical realization of quantum logic gate

(1) We prepare the physical system in the well-defined initial quantum state $|\Psi(0)\rangle = |input\rangle$ at the initial time instant $t = 0$.

(2) We apply the controlled perturbation $H_{int}(t)$ with time duration T to the system.
total Hamiltonian: $H(t) = H_0 + H_{int}(t)$.
During the time interval $0 \leq t \leq T$, the quantum system evolves according to $|\Psi(t)\rangle = U(t)|\Psi(0)\rangle = \exp[(-i/\hbar)Ht]|\Psi(0)\rangle$.

(3) We measure the final quantum state at time $t = T$

$$|\Psi(T)\rangle = |output\rangle = U(T)|input\rangle \ .$$

3.2 Single qubit logic gates

The single qubit (one-qubit) logic gate transforms the initial (input) qubit into the target (output) qubit.

Example: NOT gate

$$U_{\rm NOT} \equiv \sigma_x = \begin{pmatrix} 0 & 1 \\ 1 & 0 \end{pmatrix} \tag{15}$$

$$U_{\rm NOT} \begin{pmatrix} a_0 \\ a_1 \end{pmatrix} = \begin{pmatrix} a_1 \\ a_0 \end{pmatrix} \tag{16}$$

$\Longrightarrow$ The NOT gate interchanges the basis qubits: $|0\rangle \longleftrightarrow |1\rangle$.

3.3 Multiple qubit gates

Example of double qubit gate: Controlled NOT gate (CNOT)

Outcomes of controlled NOT gate ($U_{\rm CNOT}$) acting on two-qubit basis states

$$\begin{aligned} U_{\rm CNOT}|00\rangle &= |00\rangle \ , & \text{(17a)} \\ U_{\rm CNOT}|01\rangle &= |01\rangle \ , & \text{(17b)} \\ U_{\rm CNOT}|10\rangle &= |11\rangle \ , & \text{(17c)} \\ U_{\rm CNOT}|11\rangle &= |10\rangle \ . & \text{(17d)} \end{aligned}$$

$\Longrightarrow$ CNOT gate is the NOT gate for the second qubit (target qubit) if and only if the first qubit (control qubit) is in state $|1\rangle$.

3.3.1 Creating (producing) the entangled state

The CNOT gate can be used to produce the entangled state as follows:

$$U_{\rm CNOT}(\alpha|0\rangle + \beta|1\rangle)|0\rangle = \alpha|00\rangle + \beta|11\rangle \ , \tag{18}$$

where $|\alpha|^2 + |\beta|^2 = 1$

3.4 SWAP gate

The SWAP gate interchanges the two qubits

$$U_{\mathrm{SWAP}}|i\rangle_A|j\rangle_B = |j\rangle_A|i\rangle_B \ . \tag{19}$$

If $|i\rangle_A, |j\rangle_B$ are the electron spin states, i.e., $|i\rangle_A|j\rangle_B \equiv |\uparrow\rangle_A|\downarrow\rangle_B$, then

$$U_{\mathrm{SWAP}}|\uparrow\rangle_A|\downarrow\rangle_B = |\downarrow\rangle_A|\uparrow\rangle_B \ . \tag{20}$$

$\Longrightarrow$ **The spins are interchanged.**

3.5 Universal set of quantum logic gates

Universal set of quantum logic gates consists of all one-qubit gates and the single CNOT gate.

$\Longrightarrow$ Arbitrary quantum logic gate operating on the multiple qubit state is equivalent to a suitable combination of one-qubit gates and the CNOT gate.

3.6 Quantum Computing with Quantum Dots

We expect that **the electrostatic QD's (gate defined QD's)** should be the most appropriate nanodevices to the physical realization of qubits and quantum logic gates.

Qubits in QD's:

- charge qubit (two orbital quantum states of the electron confined in the QD)
- spin qubit (two spin eigenstates of z spin component of electron)

4 Simulation of CNOT gate on coupled QD's

S. Moskal, S. Bednarek, J. Adamowski, Phys. Rev. A 71 (2005) 062327.

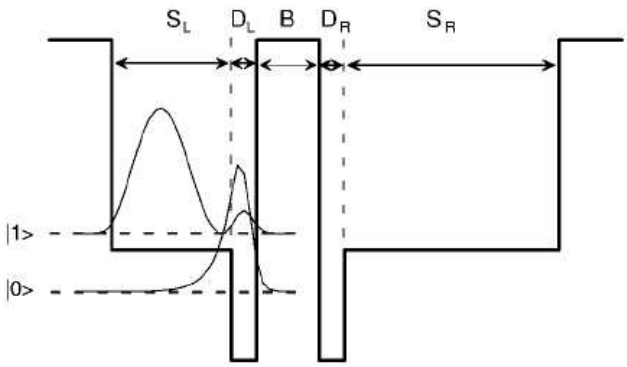

FIG. 1. Confinement potential profile in the vertical direction for two coupled QDs. Shown is also the electron probability density for the one-electron ground ($|0\rangle$) and first excited ($|1\rangle$) states. B is the barrier thickness, D_L (D_R) is the thickness of the deep potential-well region in the left (right) QD, and S_L (S_R) is the thickness of the shallow potential-well region in the left (right) QD.

Figure 1: Confinement potential profile for coupled asymmetric QD's.

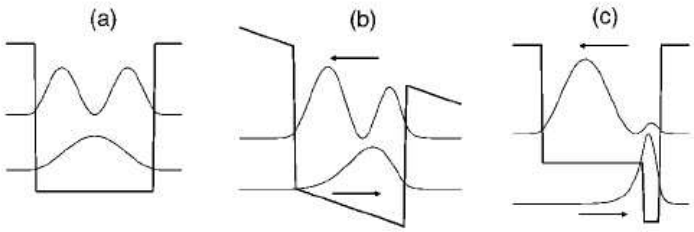

FIG. 2. Electron probability density for the one-electron ground and first excited states localized in (a) symmetric QD, (b) symmetric QD in an electric field, and (c) asymmetric QD. Arrows indicate the shift of the electron density in cases (b) and (c) with respect to case (a).

Figure 2: Effects of electrostatic field and confinement potential asymmetry on electron states in QD's.

Figure 3: Rabi oscillations $P_i(t)$ and electron probability density contours as functions of time for single qubit states $|0\rangle$ and $|1\rangle$.

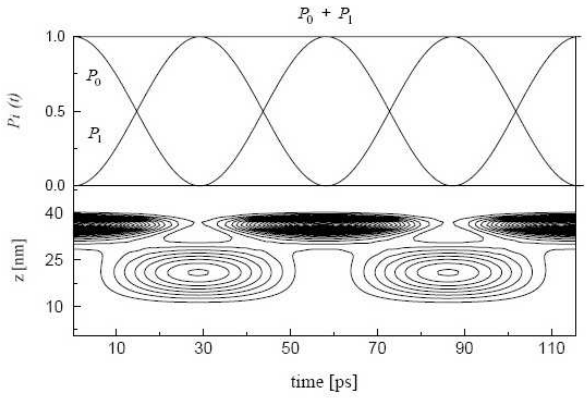

- We study the two-electron system in spin singlet state confined in double coupled asymmetric QD's.
- We assume that the lateral degrees of freedom (x, y) are "frozen": $\Longrightarrow$ effective 1D problem.
- We switch on/off the interaction $H_{int}(t)$ with electromagnetic wave for time $T = T_\pi$

  $$H_{int}(t) = A\cos(\omega t)(\hat{p}_1 + \hat{p}_2) \ ,$$

  where $\hat{p}_1$ and $\hat{p}_2$ are the electron momentum operators.
- π pulse with the duration time

  $$T_\pi = \pi \frac{\hbar |\langle 10|(\hat{p}_1 + \hat{p}_2)|11\rangle|}{A}$$

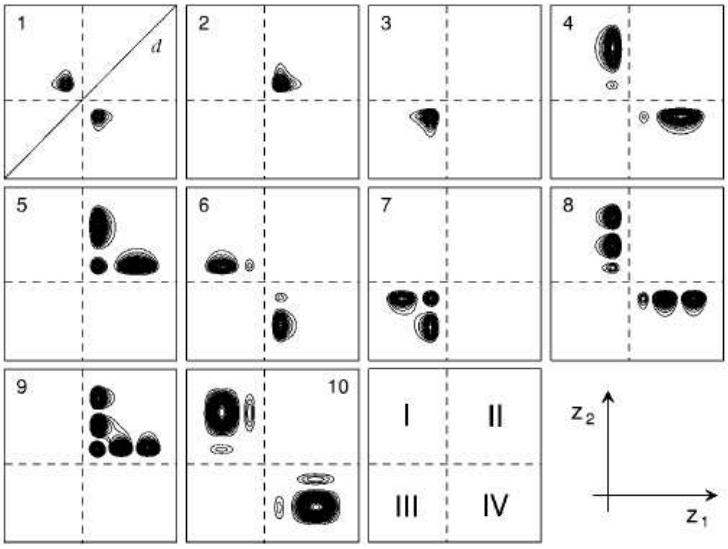

Figure 4: Contours of electron probability density for ten low-energy two-electron states. States 1, 4, 6, and 10 have been chosen as the computational basis.

$$\rho_1(z_1,t) = \int_{-\infty}^{+\infty} dz_2 \rho(z_1,z_2,t), \qquad (14)$$

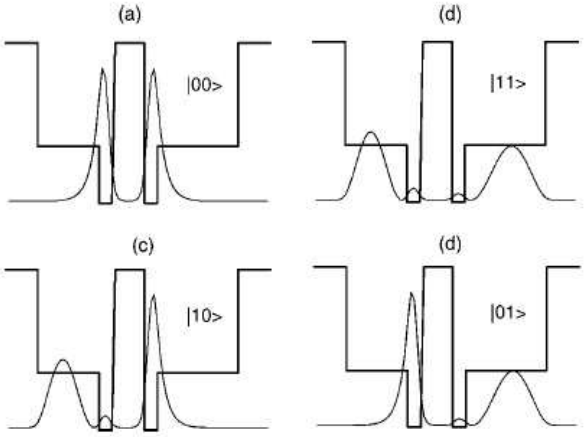

FIG. 5. One-electron probability density [Eq. (14)] for the computational-basis states for t=0. Also shown is the profile of the confinement potential.

Figure 5: One-electron probability density $\rho_1(z_1, t = 0)$ for the states of computational basis.

TABLE II: Energy levels E_ν of the ten lowest-energy states of the model two-electron system. ν numbers the subsequent energy levels. The lateral excitation energy $2\hbar\omega_\perp$ is included in E_ν. The computational-basis states $|ij\rangle$ are listed in the last column.

ν	E_ν [meV]	$\|ij\rangle$
1	-356.59	$\|00\rangle$
2	-342.15	
3	-342.02	
4	-329.81	$\|01\rangle$
5	-324.80	
6	-321.57	$\|10\rangle$
7	-313.98	
8	-307.86	
9	-301.09	
10	-293.34	$\|11\rangle$

TABLE III: Energy separations between energy levels E_{ij} of the computational-basis states $|ij\rangle$ and energy difference ΔE between the two transition energies relevant to the CNOT gate operation.

energy difference	[meV]
$\Delta E_I = E_{01} - E_{00}$	26.78
$\Delta E_{II} = E_{11} - E_{10}$	28.23
$E_{10} - E_{01}$	8.24
$E_{10} - E_{00}$	36.47
$E_{11} - E_{01}$	35.02
$\Delta E = \Delta E_{II} - \Delta E_I$	1.45

Figure 7: Energy separations between the energy levels of computational basis. The CNOT gate is realized by absorbing the photon of energy $\hbar\omega = \Delta E_{II}$.

4.1 Steps of CNOT gate

(a) Relaxation of the system to the ground state $|00\rangle$

(b) Preparation of the required initial state:

$$|00\rangle \longrightarrow |initial\rangle \equiv |ij\rangle$$

(c) Absorption of electromagnetic wave with photon energy $\hbar\omega$ and pulse duration T_π
$\Longrightarrow$ quantum transition
$|initial\rangle \longrightarrow |final\rangle = |i'j'\rangle$

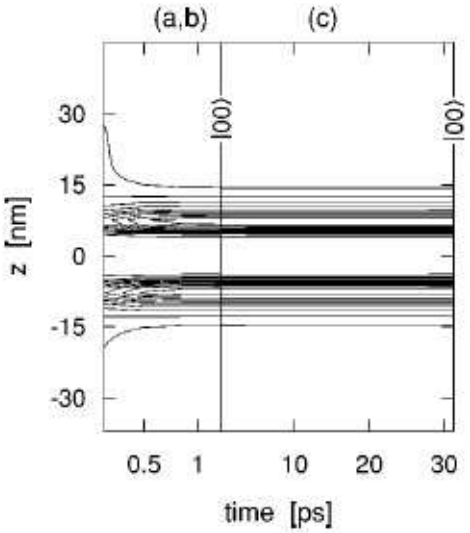

FIG. 6. Contour plots of the electron probability density as functions of time t and spatial coordinate z=z_1 for the working cycle of the CNOT gate corresponding to the operation defined by Eq. (7a). (a,b) corresponds to the relaxation of the system to the ground state and simultaneously the preparation of the initial state. (c) corresponds to the CNOT gate operation defined by Eq. (7a).

Figure 8: Computer simulation of operation $U_{\mathrm{CNOT}}|00\rangle = |00\rangle$.

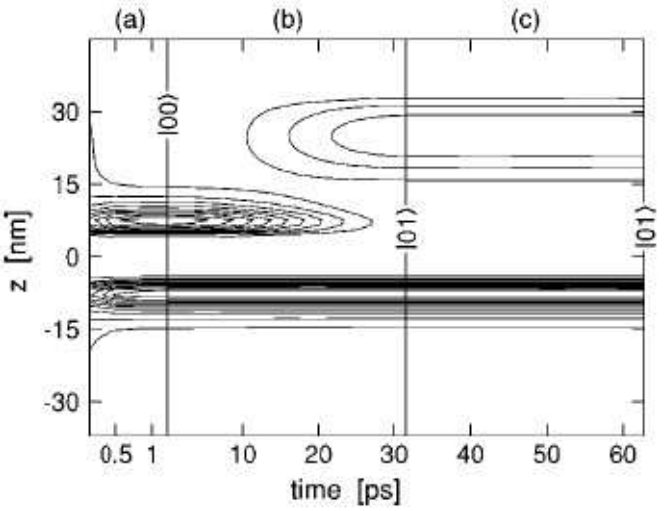

Figure 9: Computer simulation of operation $U_{\mathrm{CNOT}}|01\rangle = |01\rangle$.

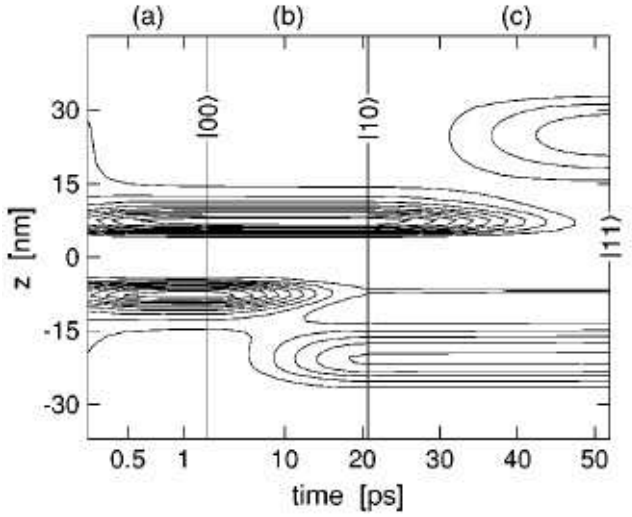

Figure 10: Computer simulation of operation $U_{\mathrm{CNOT}}|10\rangle = |11\rangle$.

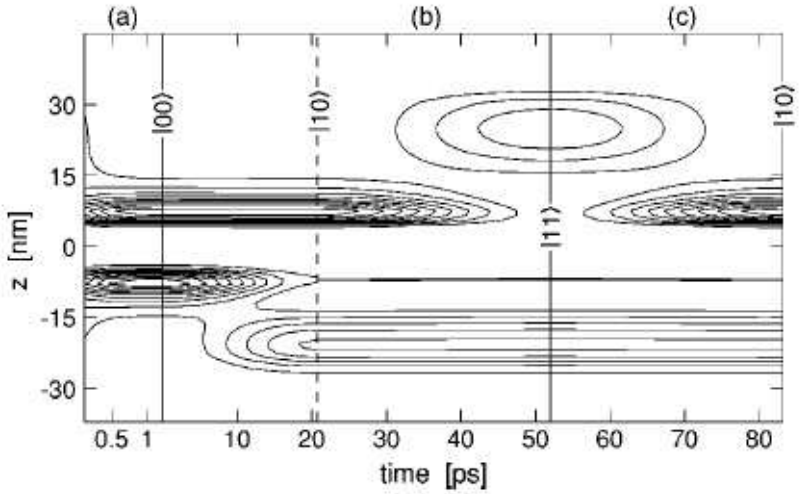

Figure 11: Computer simulation of operation $U_{\mathrm{CNOT}}|11\rangle = |11\rangle$.

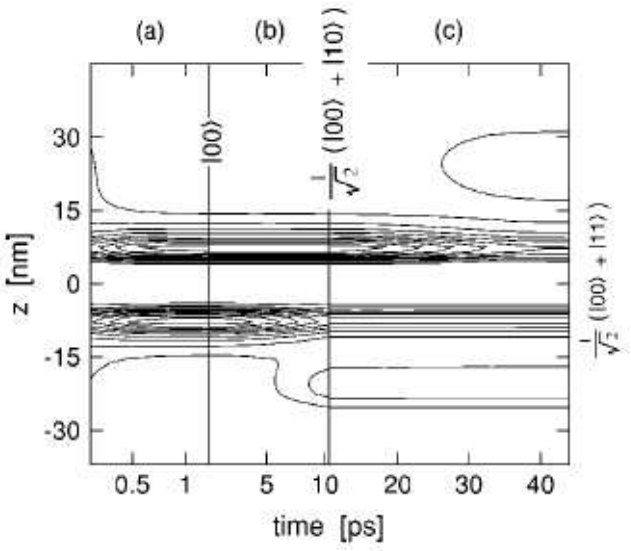

Figure 12: Production of entangled state $U_{\mathrm{CNOT}}\left(\frac{1}{\sqrt{2}}|0\rangle + \frac{1}{\sqrt{2}}|1\rangle\right)|0\rangle = \frac{1}{\sqrt{2}}(|00\rangle + |11\rangle)$.

5 Simulation of SWAP operation on electron spin qubits

S. Moskal, S. Bednarek, J. Adamowski, Phys. Rev A 76 (2007) 032302.

5.1 Interchanging the electron spins in double coupled gate-controlled QD's

Periodic changes of the gate voltage induce the following oscillations of the confinement potential:

two separate potential wells $\Longrightarrow$ single potential well $\Longrightarrow$ two separate potential wells $\Longrightarrow$ ...

The oscillating confinement potential gives rise to the tunnelling of electrons to the single common potential well and back to the separate potential wells.
$\Longrightarrow$ The electrons interchange their spins.
$\Longrightarrow$ **SWAP operation**

The proposed mechanism can be described by the effective Heisenberg Hamiltonian

$$H_{eff} = J(t)\vec{\sigma}_1 \cdot \vec{\sigma}_2 \tag{21}$$

where $J(t)$ = exchange energy
$\vec{\sigma}_1, \vec{\sigma}_2$ = Pauli spin operators

Note

$$\vec{\sigma}_1 \cdot \vec{\sigma}_2 = 2P_{12} - \mathbf{1}$$

where P_{12} = permutation operator that interchanges the particle indices $1 \longleftrightarrow 2$

$\Longrightarrow$ **The spins become interchanged with probability**

$$P = 2/3 < 1 \, .$$

5.2 Vertically coupled QD's

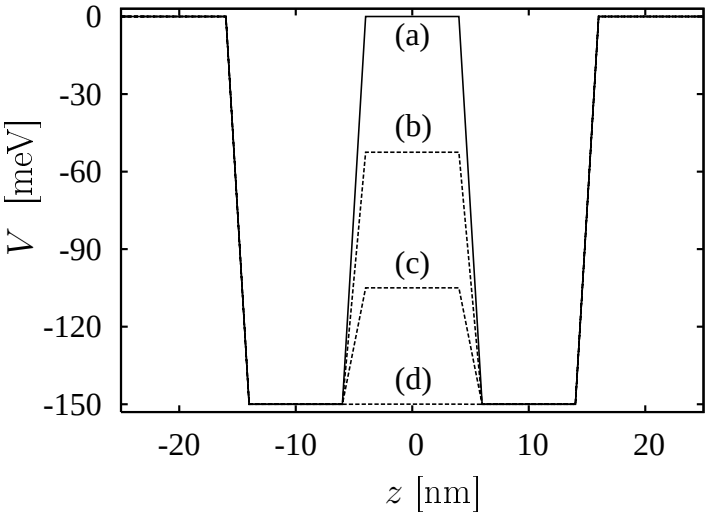

Figure 13: Potential barrier separating vertically coupled QD's.

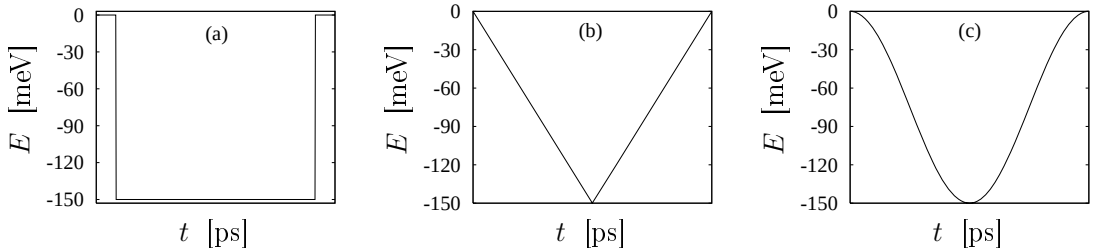

Figure 14: Time dependence of top barrier energy: (a) step function, (b) piecewise linear function, (c) smooth (cosine) function.

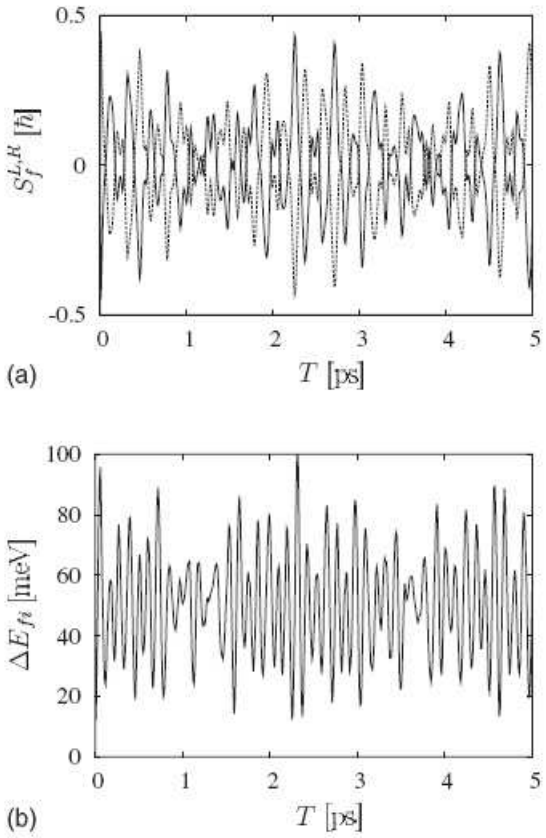

FIG. 3. (a) Expectation values $S_f^{L,R}$ of the z-spin component recorded at the end of the process of switching on and off the exchange interaction as a function of process duration time T for step like changes of the barrier. The solid (dashed) curve shows the results for an electron in the right (left) QD. (b) Energy difference ΔE_{fi} between the final- and initial-state energies as a function of process duration time T.

Figure 15: Results for step-like changes of potential barrier.

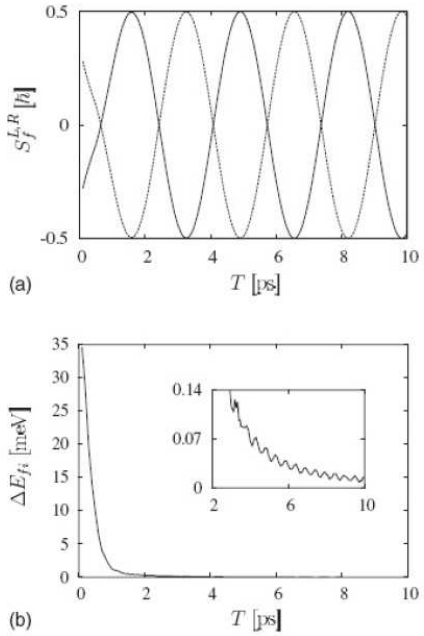

Figure 16: Results for piece-wise linear changes of potential barrier.

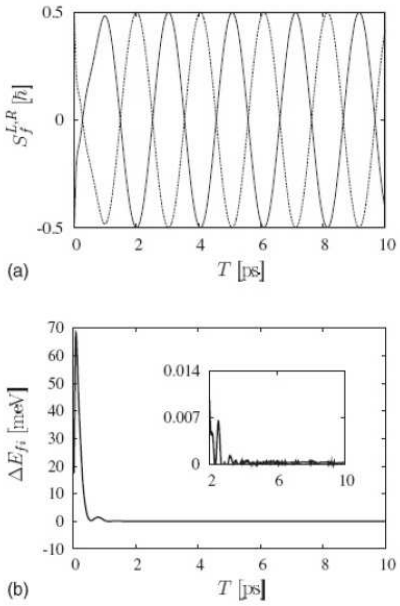

Figure 17: Results for smooth changes of potential barrier.

5.3 Laterally coupled symmetric QD's

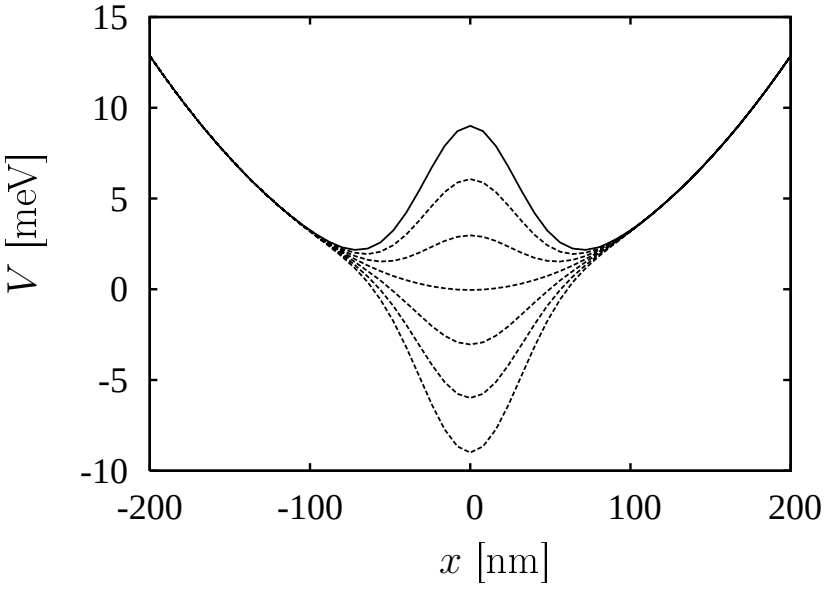

Figure 18: Time changes of confinement potential profile.

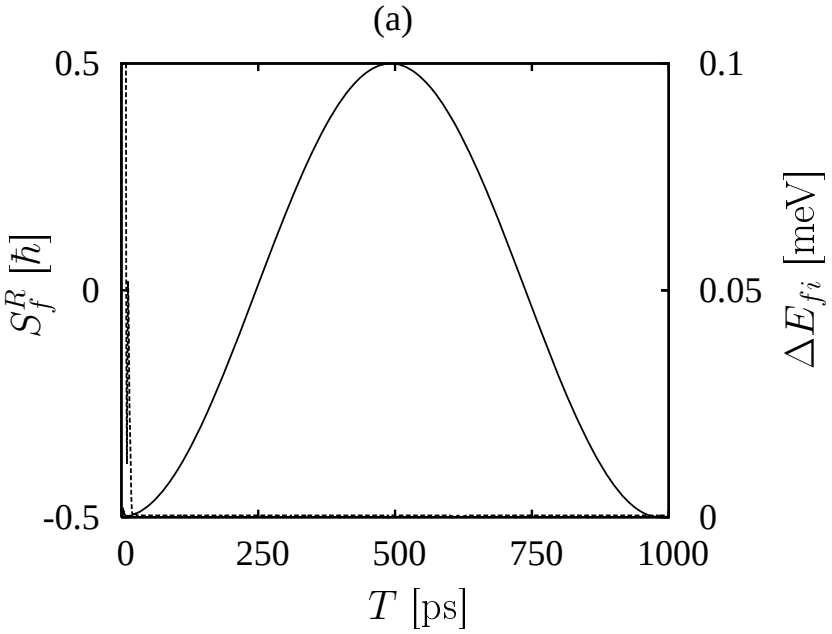

Figure 19: Expectation value S_f^R of z spin component for electron final state in the right QD (solid curve) and energy difference ΔE_{fi} between the final and initial states as functions of time duration T of the process. (a) $V_{min} = 0$.

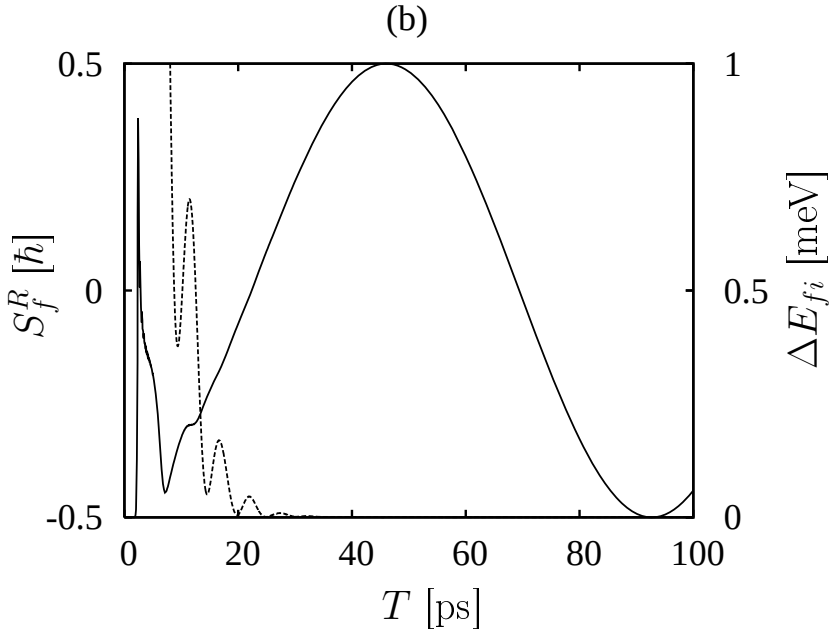

Figure 20: (b) $V_{min} = -3$ meV.

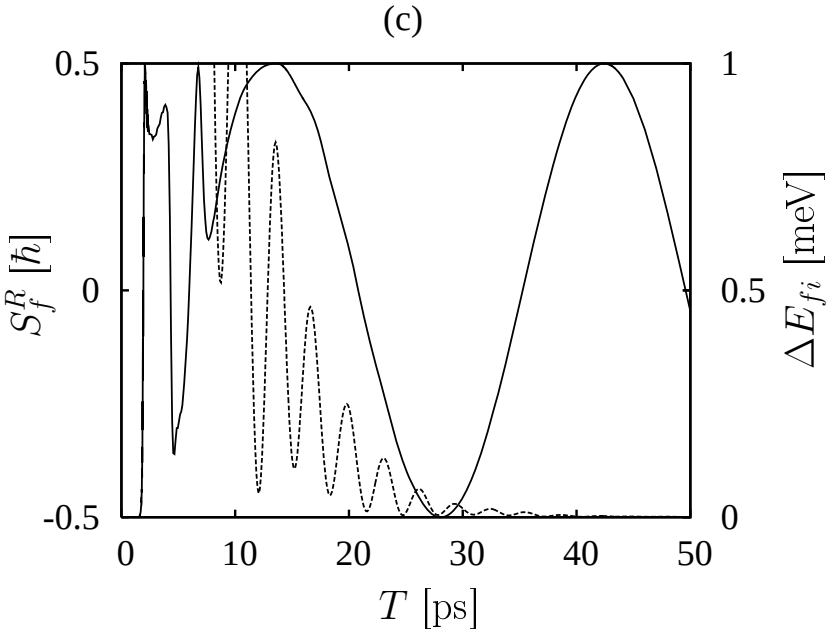

Figure 21: (c) $V_{min} = -6$ meV.

5.4 Laterally coupled asymmetric QD's

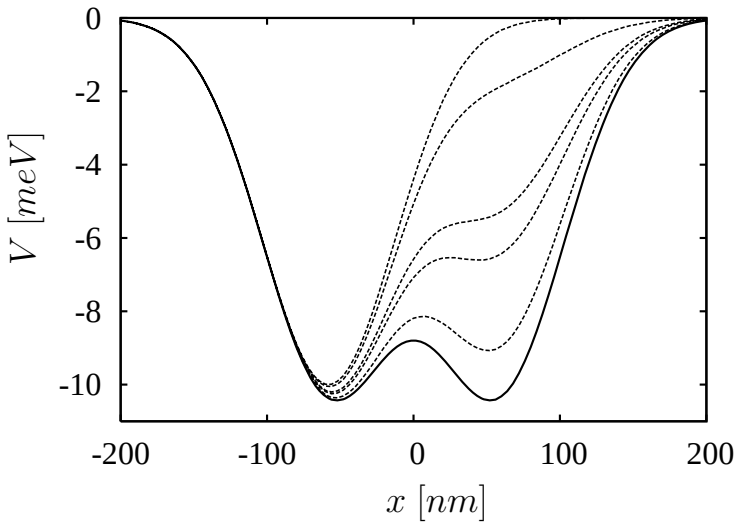

Figure 22: Confinement potential profile for several time instants.

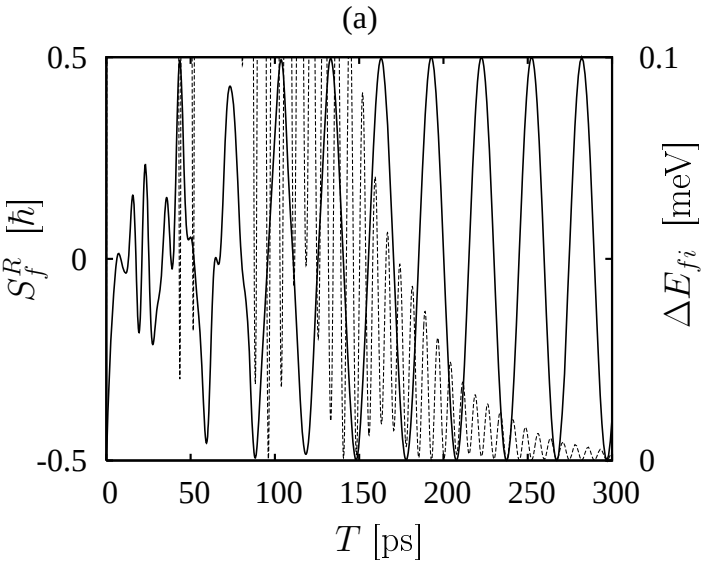

Figure 23: Expectation value S_f^R of z spin component for electron final state in the right QD (solid curve) and energy difference ΔE_{fi} between the final and initial states as functions of time duration T of potential changes. (a) $V_{max}^R = -3$ meV.

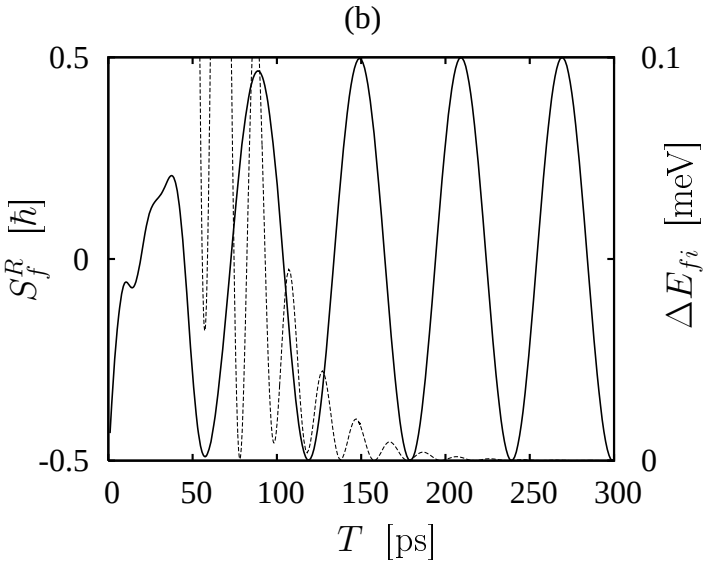

Figure 24: (b) $V_{max}^R = -5$ meV.

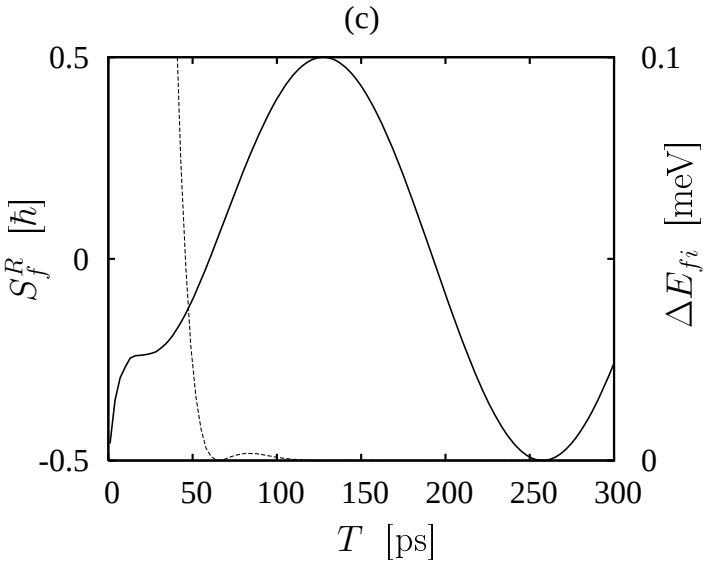

Figure 25: (c) $V_{max}^R = -6$ meV.

The results of simulations show that – in general – the electron spin swapping occurs **several times** before the full interchange of spins is reached.

$\Longrightarrow$ **Elongation of the gate operation time.**

6 Discussion

Conditions for physical realization of quantum logic gates

(1) Physical realizability of qubits

(2) Precise preparation of initial (input) qubit

(3) Operation time has to be very short
($\sim 10^4$ times shorter than the decoherence time)

(4) Controlled time evolution of the system

(5) Accurate measurement of final (output) qubit

(6) Scalability (many qubits are required for the storage and processing of information)

6.1 Problems

(1) Decay of the excited quantum state
T_1 = relaxation time

(2) Decoherence
T_2 = coherence time

Usually, $T_2 < T_1$.For spin qubits in semiconductors: $T_1 \geq 50\mu$s and $T_2 \simeq T_1$.

The main reason of **relaxation of spin qubits in semiconductors:**hyperfine interaction of electron spin with the spins of nuclei of crystal lattice.

Spin I of nucleus:

$I = 3/2$ for Ga and As, e.g., in GaAs
$I = 9/2$ for In, e.g., in InAs, InP
But $I = 0$ for ^{28}Si.

Decoherence

Change of **relative phase** of basis qubits due to unavoidable interactions with the surrounding.

$$|\psi\rangle = a_0|0\rangle + a_1|1\rangle \longrightarrow a_0|0\rangle + e^{i\theta}a_1|1\rangle \tag{22}$$

where θ = **relative phase shift** that changes the expectation values of measured quantities
Decoherence is the main effect of destroying the quantum information.

Approximate measure of the quality of quantum processor

$$R = \frac{T_2}{T_{operation}} \tag{23}$$

Optimal values of R that are required for multiple error corrections

$$1000 \leq R \leq 10000$$

Main sources of decoherence

(1) Electron-phonon interaction
$\Longrightarrow$ decoherence of orbital (charge) qubits
(coherence time $T_2 \simeq 1 - 10$ ns)

(2) Hyperfine interaction of electron spin with nuclear spins
$\Longrightarrow$ decoherence of spin qubits ($T_2 \simeq 1\mu$s)

6.2 Experiments with spin qubits

6.2.1 Non-destructive measurement of spin for electron pair in single QD

T. Meunier et al., Phys. Rev. B 74 (2006) 195303.

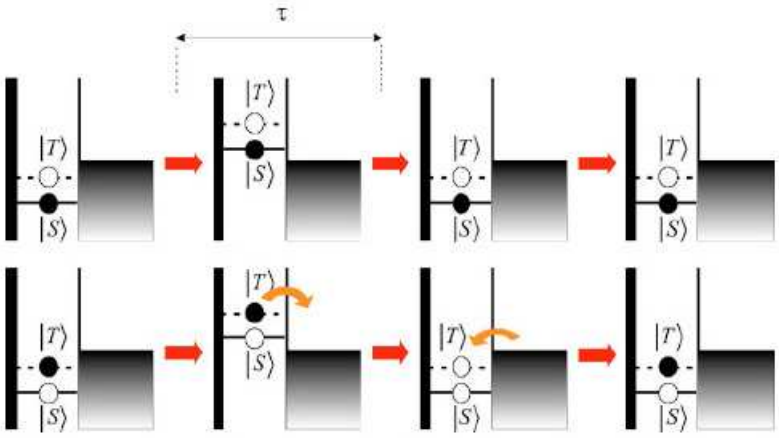

FIG. 1. (Color online) Schematic of the quantum dot throughout the nondestructive measurement scheme, for a singlet (top) or triplet (bottom) initial state. Curved arrows indicate tunnel process. The interesting feature is that the spin state is the same before and after the measurement.

Figure 26: Schematic of measurement.

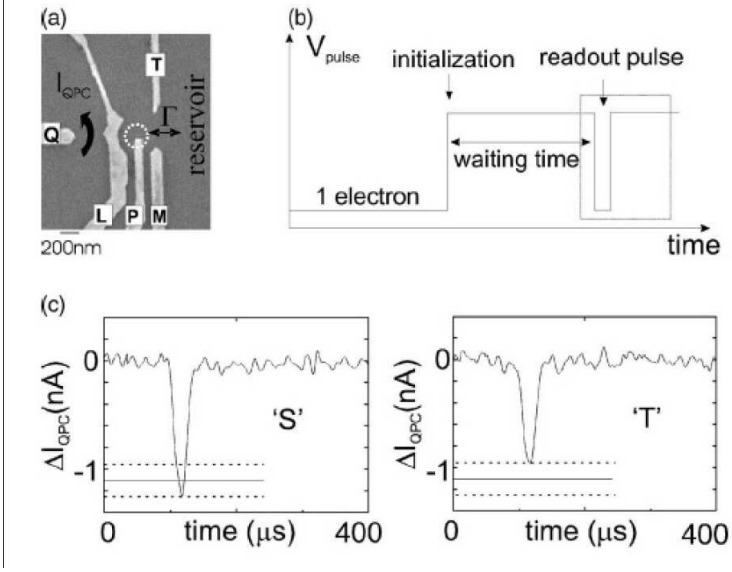

Figure 27: (a) Scanning electron microscope image. (b) Pulses of voltage applied to gate P. (c) Change of current detected by a Quantum Point Contact (QPC) during time interval 400 μs as a response to signal labelled by the rectangle in (b) for singlet 'S' and triplet 'T'.

6.2.2 Coherent manipulation with spin qubits in coupled QD's

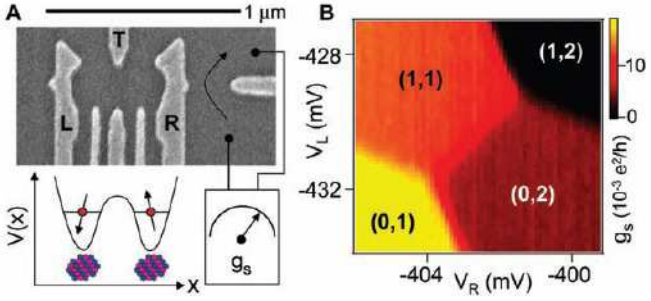

Fig. 1. (A) Scanning electron micrograph of a sample identical to the one measured, consisting of electrostatic gates on the surface of a two-dimensional electron gas. Voltages on gates L and R control the number of electrons in the left and right dots. Gate T is used to adjust the interdot tunnel coupling. The quantum point contact conductance g_s is sensitive primarily to the number of electrons in the right dot. (B) g_s measured as a function of V_L and V_R reflects the double-dot charge stability diagram (a background slope has been subtracted). Charge states are labeled (m,n), where m is the number of electrons in the left dot and n is the number of electrons in the right dot. Each charge state gives a distinct reading of g_s.

MBER 2005 VOL 309 SCIENCE www.sciencemag.org

Figure 28: (A) Gate electrodes defining the QD, confinement potential profile, and schematic of conductivity measurement. (B) Results of conductivity measurements for different numbers (n, m) of electrons in the left (n) and right (m) QD.

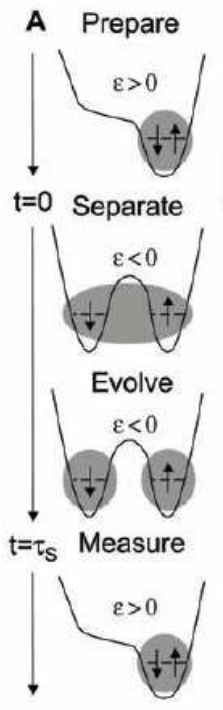

Figure 29: Cycles of spin manipulation by changing the asymmetry parameter ε that determines the difference between the voltages applied to electrodes L and R.

7 Summary

Present status of research and technology

$\Longrightarrow$ Second Quantum Revolution • quantum technologies (developing since $\sim$1990)

First Quantum Revolution

It lasted since 1900 (Max Planck) until $\sim$ 1940 (Richard Feynman).

During that time the quantum laws had been formulated, the fundamental quantum phenomena had been discovered and explained.

The formulation of quantum laws in terms of path integrals by Richard Feynman ($\sim$ 1942) is treated as the end of the first quantum revolution.

On the 29th December 1959, in Caltech, the same Richard Feynman gave a lecture entitled:
„There is plenty of room at the bottom"

[published in Engineering and Science, Caltech, Vol. XXIII (1960) p. 22]

In this lecture, Richard Feynman proposed a direct application of single atoms and molecules to the storage of information.

Developing quantum technologies

- quantum storage of information
- quantum computational algorithms
- quantum cryptography
- quantum teleportation
- coherent quantum electronics: coherent electron currents
- quantum optics: single photon sources
- nanoelectronics: single electron transistor
- spintronics: spin transistor
- single electron memory cell
- quantum lithography
- atom laser: coherent atomic and molecular beams
- molecular electronics

Towards a quantum computer

- Advanced stage of theory of quantum computation
  $\Longrightarrow$ quantum algorithms

- Promising results of experimental manipulation of spin qubits
- Unfortunately, the physically optimal realization of quantum computer has not been established yet:
  quantum dots, superconducting circuits, ionic traps, atomic cavities, NMR systems, ...

Competitive technologies

(1) ionic traps

(2) atomic cavities

(3) NMR systems

(4) superconducting circuits

Disadvantages of systems (1-3)

- hard integrability with recent electronics
- hard scalability
- large sizes

Advantages of quantum dots

(1) Possibility of modelling the electronic properties
$\Longrightarrow$ **quantum engineering**

(2) Easy integration with the existing electronics
$\Longrightarrow$ **nanoelectronics**

(3) Scalability
integrated system = array of QD's

(4) Limit of miniaturization of man-made electronic devices
$\Longrightarrow$ **further miniaturization: application of natural atoms and molecules**
$\Longrightarrow$ **molecular electronics**